frontiers in Earth Science

ORIGINAL RESEARCH
published: 07 May 2019
doi: 10.3389/feart.2019.00085

Diazotrophy Drives Primary Production in the Organic-Rich Shales Deposited Under a Stratified Environment During the Messinian Salinity Crisis (Vena del Gesso, Italy)

Yuta Isaji[1], Hodaka Kawahata[2], Yoshinori Takano[1], Nanako O. Ogawa[1], Junichiro Kuroda[2], Toshihiro Yoshimura[1], Stefano Lugli[3], Vinicio Manzi[4], Marco Roveri[4] and Naohiko Ohkouchi[1]*

[1] Department of Biogeochemistry, Japan Agency for Marine-Earth Science and Technology, Yokosuka, Japan, [2] Atmosphere and Ocean Research Institute, The University of Tokyo, Kashiwa, Japan, [3] Dipartimento di Scienze Chimiche e Geologiche, Università degli Studi di Modena e Reggio Emilia, Modena, Italy, [4] Dipartimento di Scienze Chimiche, della Vita e della Sostenibilità Ambientale, University of Parma, Parma, Italy

Density stratification between freshwater and brine is periodically formed during massive evaporation events, which often associates deposition of organic-rich sediments. Here, we investigated phototrophic communities and nitrogen cycle during the deposition of two organic-rich shale beds of gypsum–shale alternation, representing the initial stage of the Messinian salinity crisis (Vena del Gesso, Northern Apennines, Italy). The structural distributions and the carbon and nitrogen isotopic compositions of geoporphyrins show a common pattern in the two shales, indicating the predominance of a particular phototrophic community under freshwater–brine stratified conditions. The ~6‰ difference in $\delta^{13}C$ of total organic carbon between PLG 4 and 5 shales was associated with similar shift in $\delta^{13}C$ of the porphyrins derived from chlorophyll *c*, suggesting that the eukaryotic algae producing chlorophyll *c* were the major constituent of the phototrophic community. Importantly, these porphyrins show $\delta^{15}N$ values (−7.6–−4.7‰) indicative of N_2-fixation. We suggest that nitrate-depletion in the photic zone induced the predominance of diazotrophic cyanobacteria, which supplied new nitrogen for the chlorophyll *c*-producing eukaryotic algae. The large difference in the $\delta^{13}C$ values of porphyrins and total organic carbon between PLG 4 and 5 shales are interpreted to reflect the depth of the chemocline, which fluctuates in response to changes in the regional evaporation–precipitation balance. Such variation in the chemocline depth may have dynamically changed the mode of the nitrogen cycle (i.e., nitrification–denitrification–N_2-fixation coupling vs. phototrophic assimilation of ammonium) in the density-stratified marginal basins during the Messinian salinity crisis.

Keywords: Messinian salinity crisis, organic-rich shale, density stratification, N_2-fixation, porphyrins, carbon isotope, nitrogen isotope

OPEN ACCESS

Edited by:
Moritz Felix Lehmann, Universität Basel, Switzerland

Reviewed by:
Stefano Michele Bernasconi, ETH Zurich, Switzerland
Felix J. Elling, Harvard University, United States

****Correspondence:***
Yuta Isaji
isajiy@jamstec.go.jp

Specialty section:
This article was submitted to Biogeoscience, a section of the journal Frontiers in Earth Science

Received: *28 January 2019*
Accepted: *08 April 2019*
Published: *07 May 2019*

Citation:
Isaji Y, Kawahata H, Takano Y, Ogawa NO, Kuroda J, Yoshimura T, Lugli S, Manzi V, Roveri M and Ohkouchi N (2019) Diazotrophy Drives Primary Production in the Organic-Rich Shales Deposited Under a Stratified Environment During the Messinian Salinity Crisis (Vena del Gesso, Italy). Front. Earth Sci. 7:85. doi: 10.3389/feart.2019.00085

Abbreviations: BiCAP, bicycloalkanoporphyrin; DDAs, diatom–diazotrophic associations; DIC, dissolved inorganic carbon; DPEP, deoxophylloerythroetioporphyrin; HPLC/APCI–MS, high-performance liquid chromatography/atmospheric pressure chemical ionization–mass spectrometry; MSC, Messinian salinity crisis; NMR, nuclear magnetic resonance; PLG, Primary Lower Gypsum; TOC, total organic carbon.

INTRODUCTION

Density stratification between water masses having distinct salinity is commonly formed in hypersaline environments. In particular, stratification between freshwater and brine is periodically formed during past massive evaporation events, which is known to have occurred repeatedly in the geological past (Hay et al., 2006; Warren, 2010). Formation of surface freshwater layer must have resulted in temporal relief of organisms from salinity stress and the formation of anoxic bottom water mass, which substantially modify the biogeochemical cycle and thus its global influence. Indeed, such environmental condition is often associated with the deposition of organic-rich sediments, which intercalate evaporite beds synchronous with climatic oscillations (Warren, 2016). To understand the evolution and consequences of the massive evaporation events, it is essential to reveal the biogeochemical cycle of freshwater-brine stratified condition.

At end of the Miocene, between 5.97 and 5.33 Ma, the Mediterranean Sea experienced one of the greatest evaporation events in the Earth's history, known as the Messinian salinity crisis (MSC; Hsü et al., 1973; Krijgsman et al., 1999; Rouchy and Caruso, 2006; Ryan, 2009; Roveri et al., 2014, and references therein). During the first stage of the MSC (5.97-5.60 Ma), up to 16 lithological cycles, given by the superposition of thin organic-rich shale or marl and tens of meters-thick primary bottom-grown gypsum beds ($CaSO_4 \cdot 2H_2O$), were deposited in the marginal shallow (<200 m) basins of the Mediterranean (**Figure 1**, Primary Lower Gypsum: PLG; Lugli et al., 2010). These cycles record a ∼21 kyr precession-driven alternation of climatic and paleoceanographic conditions; arid climate phase precipitating gypsum punctuated by inflows of continental freshwater during the humid climate phase causing water column stratification and the deposition of organic-rich shales (Lugli et al., 2010).

The representative PLG section outcrops in the Vena del Gesso basin of the Northern Apennines, Italy (Lugli et al., 2010; Roveri et al., 2014). Biomarkers indicative of phototrophs such as diatoms, dinoflagellates, and cyanobacteria have been reported from these PLG shales, as well as isorenieratane derived from green sulfur bacteria which suggests periodical intrusion of euxinic water masses into the photic zone (Keely et al., 1995; Kenig et al., 1995; Schaeffer et al., 1995; Sinninghe Damsté et al., 1995). Determining the dominant primary producer among these phototrophs is of critical importance, as the composition of phototrophic community is intimately related to the efficiency of export production (Berger et al., 1989; Honjo et al., 2008). Accordingly, it is also necessary to reveal the nutrient dynamics of the system, because its availability is a fundamental controlling factor for the composition and primary productivity of the phototrophic community. However, extraction of marine signal is complicated by the presence of considerable amount of terrigenous organic matter in the PLG shales (Sinninghe Damsté et al., 1995).

Geoporphyrins are tetrapyrrole molecules derived mainly from chloropigments (i.e., chlorophylls and bacteriochlorophylls) that are preserved in sediments on a geological timescale. Previous investigations have revealed precursor–product relationships between chloropigments and geoporphyrins (summarized in Treibs, 1936; Baker and Louda, 1986; Callot and Ocampo, 2000; Keely, 2006). Moreover, the carbon and nitrogen isotopic compositions of geoporphyrins retain the original signals of the chloropigments, which strongly reflect those of the source phototrophs (Sachs et al., 1999; Ohkouchi et al., 2006, 2008; Higgins et al., 2011). Therefore, structural and isotopic information of geoporphyrins in the geological samples provide us insights into phototrophic community as well as carbon and nitrogen cycles of past environments (Hayes et al., 1987; Boreham et al., 1989, 1990; Ocampo et al., 1989; Popp et al., 1989; Chicarelli et al., 1993; Keely et al., 1994; Ohkouchi et al., 2006, 2015; Kashiyama et al., 2008a,b, 2010; Higgins et al., 2012; Junium et al., 2015; Gueneli et al., 2018; Isaji et al., 2019). Importantly, geoporphyrins in marine sediments are mostly derived from marine phototrophs, because the turnover rate of aquatic chlorophylls are substantially faster than that of terrestrial chlorophylls (Hendry et al., 1987), and most chlorophylls produced by the terrestrial plants are enzymatically decomposed during senescence of the leaf (e.g., Matile et al., 1996), degraded by bacteria in soils (Hoyt, 1966), and readily oxidized during transport (Sanger, 1988).

This study focuses on two shale beds of the PLG sequence in the Vena del Gesso basin, deposited during the initial stage of the MSC. We identified the structures and determined carbon and nitrogen isotopic composition of individual geoporphyrins in each shale bed, which provided information on the dominant phototrophs and the carbon and nitrogen cycles during their deposition. The nitrogen cycle is of particular importance in stratified environments, as the combination of aerobic (e.g., nitrification) and anaerobic processes [e.g., denitrification, anaerobic ammonium oxidation (anammox)] has the potential to dynamically change the availability of nitrogenous nutrients (e.g., NO_3^-, NH_4^+, dissolved organic nitrogen) in the photic zone (e.g., Brandes et al., 2007). The results provide fundamental insights into the biogeochemical cycle of a density-stratified condition, which occurred widely and repeatedly in the Mediterranean Sea during the salinity crisis.

MATERIALS AND METHODS

Geological Setting and Sample Description

The Monte Tondo quarry is located in Vena del Gesso basin (Northern Apennines, Italy; **Figure 1**), where the evaporitic sequence consists of 16 cycles of thick gypsum beds (up to 30 m) intercalated with thinner organic-rich shale beds (<1 m; Lugli et al., 2010). The facies association and Sr isotope record suggest that the Vena del Gesso succession was deposited in a restricted marginal basin of the circum-Mediterranean Basin, in water depth of less than 200 m, where the oceanographic conditions were strongly affected by continental inflow (Lugli et al., 2010). The precipitation of gypsum occurred during the arid climate phase of the ∼21 kyr precessional cycle, which was interrupted by continental water inflow during the humid climate phase, resulting in water column stratification and the deposition

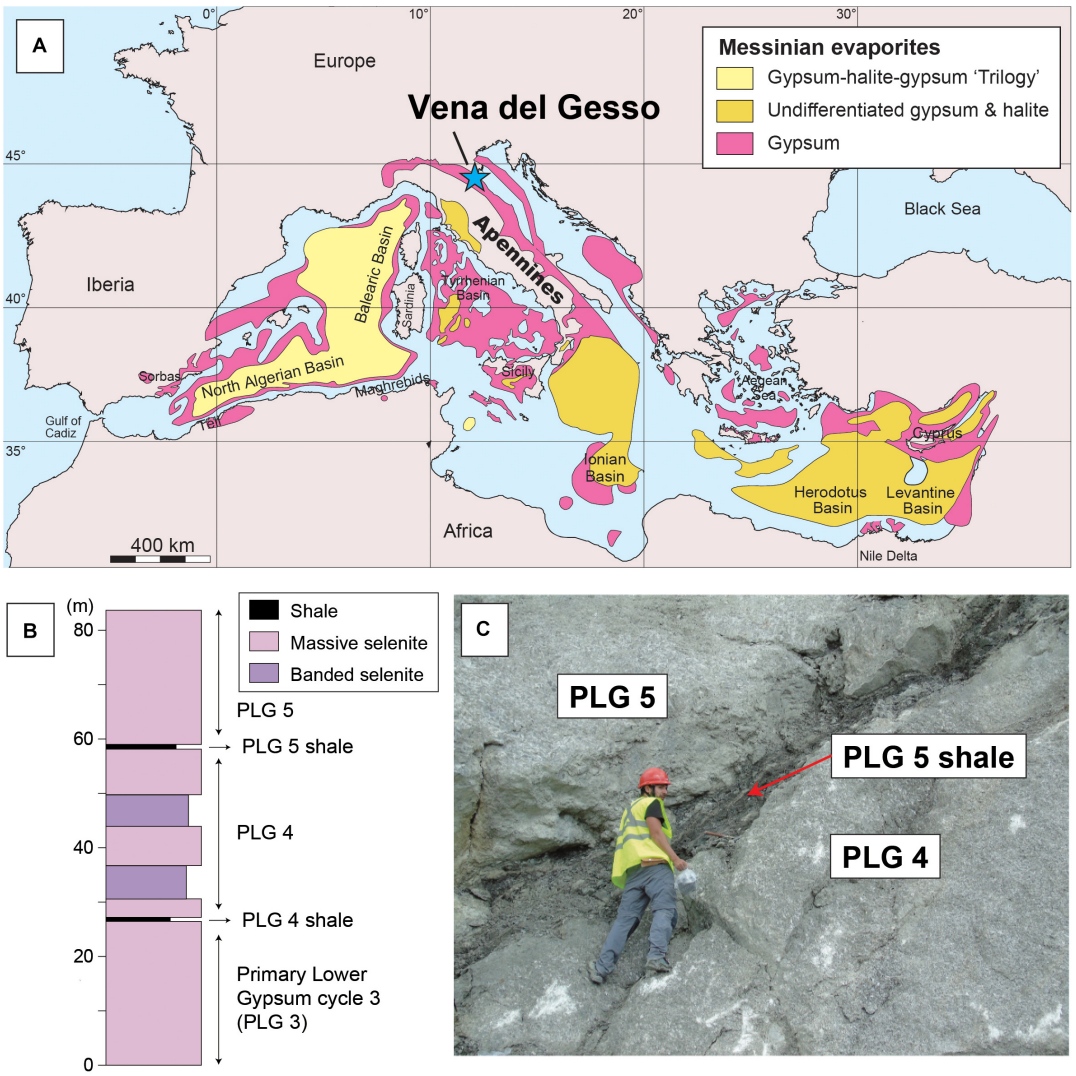

FIGURE 1 | (A) Map of the Mediterranean Sea showing the distributions of Messinian evaporites (after Ryan, 2009; Manzi et al., 2012). Samples were collected from the Monte Tondo quarry of the Vena del Gesso. **(B)** Stratigraphic column of cycles 3, 4, and 5 of the Primary Lower Gypsum (PLG) deposited during the Messinian salinity crisis. The shales analyzed in this study were deposited during the humid climate phases of the insolation maxima. Modified after Lugli et al. (2010). **(C)** The boundary between the 4th and 5th cycles at the Monte Tondo quarry of the Vena del Gesso. Samples were collected from the middle part of the shale beds. Written informed consent was obtained from the individual for the publication of this image.

of organic-rich shales (Krijgsman et al., 1999; Lugli et al., 2010; Reghizzi et al., 2018).

Gypsum beds of each cycle in the PLG are numbered from cycle 1 at the bottom to cycle 16 at the top (Lugli et al., 2010). We sampled shale beds in the PLG section at the base of cycles 4 and 5 (herein referred to as the PLG 4 and PLG 5 shales, respectively; **Figures 1B,C**). Each sample was taken from the middle part of the shale bed.

Analytical Procedures

Isolation and Purification of Geoporphyrins

The experimental procedures used in this study were modified from those reported by Kashiyama et al. (2007). Geoporphyrins in pulverized sediment samples (PLG 4 shale: ~500 g, PLG 5 shale: ~200 g) were extracted five times with dichloromethane:methanol (7:3, v/v) by sonication for 15 min. The extract was then separated with silica gel column chromatography. The low-polarity fraction was collected with dichloromethane and the polar fraction was collected using a mixture of dichloromethane and an increasing proportion of methanol. Nickel boride was added to the polar fraction to release the sulfur-bound compounds, following the methods of Schouten et al. (1993). The released sulfur-bound fraction was then separated again into low-polarity and polar fractions with silica gel column chromatography. Then, the low-polarity fraction was further separated into six sub-fractions again using silica gel column chromatography, which was deactivated with 1 wt.% of H_2O. The nickel alkylporphyrin fraction,

which was evident as a pink-colored band, was collected using *n*-hexane:dichloromethane (1:1, v/v). Prior to analysis with high-performance liquid chromatography (HPLC), the Ni alkylporphyrin fraction was passed through a C_{18} column using *N*,*N*-dimethylformamide as the mobile phase.

The individual Ni alkylporphyrins were isolated and purified with dual-step HPLC analysis. A reverse-phase HPLC analysis (Agilent 1260 series, Agilent Technologies, Santa Clara, CA, United States) was performed using an Agilent Zorbax SB-C_{18} column (4.6 mm × 500 mm; 5 μm silica particle size) with a guard column (4.6 mm × 12.5 mm; 5 μm silica particle size). The porphyrins were eluted isocratically with acetonitrile:*N*,*N*-dimethylformamide:pyridine:acetic acid (80:20:0.5:0.5, v/v/v/v) at a flow rate of 1 mL min^{-1} and a column temperature of 20°C. A photodiode-array detector was used to detect the porphyrins and each peak was collected with a fraction collector. Further purification of the collected peaks was achieved by normal-phase HPLC analysis (Agilent 1200 series, Agilent Technologies) with an Agilent Zorbax SIL column (4.6 mm × 500 mm; 5 μm silica particle size) with a guard column (4.6 mm × 12.5 mm; 5 μm silica particle size). The mobile phase for the isocratic analysis was *n*-hexane:acetone:pyridine:acetic acid (96:3:0.5:0.5, v/v/v/v) at a flow rate of 1 mL min^{-1}. The column temperature was 10°C for peaks 1, 2, and 6, and 15°C for peaks 3, 4, and 5.

Stable Carbon and Nitrogen Isotopic Compositions

The stable carbon and nitrogen isotopic compositions of the individual geoporphyrins and bulk sediments were determined with a sensitivity-enhanced Flash EA1112 elemental analyzer connected to a Thermo Finnigan Delta plus XP IRMS via a ConFlo III Interface (Ogawa et al., 2010). The purified porphyrins were dissolved in trichloromethane, transferred to pre-cleaned, smooth-wall tin capsules, and the solvents were carefully dried before analysis. The carbon and nitrogen isotopic compositions are expressed as conventional δ notation relative to VPDB and AIR, respectively. The analytical precisions for the porphyrin isotopic measurements, determined based on replicate measurements of Ni-octaethylporphyrin ($\delta^{15}N = +0.86‰$, $\delta^{13}C = -34.17‰$) as our laboratory standard, were within ±0.3‰ for $\delta^{13}C$ and ±0.8‰ for $\delta^{15}N$. For the bulk measurements, the deposits were powdered and treated with 0.1 mol L^{-1} HCl to remove $CaCO_3$ in precleaned smooth-wall tin capsules before analysis. The analytical precisions were determined based on replicate measurements of Ni-octaethylporphyrin and L-tyrosine ($\delta^{15}N = +8.74‰$, $\delta^{13}C = -20.83‰$; Tayasu et al., 2011), and were within ±0.2‰ for $\delta^{13}C$ and ±0.5‰ for $\delta^{15}N$.

Structure Assignments

The molecular structures were tentatively assigned for the compounds 1a, 1b, 3b, and 6a based on UV-Vis spectra, HPLC/MS mass spectra, and comparison with the relative retention times of those published in the literature (Sundararaman and Boreham, 1993; Kashiyama et al., 2010). The mass spectra were obtained from *m/z* 400 to 1200 with atmospheric pressure chemical ionization (APCI) mass spectrometry in positive-ion mode using an Agilent HPLC 1260 Infinity coupled to a 6460 Triple Quadrupole (QQQ) LC/MS system. The APCI conditions were set as follows: drying gas temperature: 350°C; vaporizer temperature: 500°C; drying gas flow rate: 9 L min^{-1}; nebulizer pressure: 50 psi; capillary voltage: +4000 V; and corona current: 5.0 μA. The structures of compounds 2a, 3a, 4a, and 5a purified from PLG 4 shale were identified by NMR spectroscopy. The ^1H NMR spectra were obtained using a Bruker Avance-III spectrometer operated at 400 MHz. Each compound was dissolved in $CDCl_3$ in a 1 mm i.d. tube. The chemical shifts were calibrated with the signal peaks of $CDCl_3$.

RESULTS

Distribution of Geoporphyrins

The structural distribution of sulfur-bound Ni alkylporphyrin of the two shale samples were similar (**Figure 2** and **Supplementary Figures S1–S5**), indicating that similar phototrophic community prevailed during the deposition of these shales. The most abundant Ni alkylporphyrin was C_{33}-bicycloalkanoporphyrin (C_{33}-BiCAP, 5a). This is categorized as bicycloalkanoporphyrin-type (BiCAP-type), along with C_{31}-3-nor-BiCAP (3b) and C_{33}-BiCAP with a double bond at C-13^2 and C-17^3 (6a), as well as their potential analog C_{32}-15,17-cycloheptanoporphyrin (2a). They are considered to derive mainly from chlorophyllone and 13^2,17^3-cyclopheophorbide enol (Goericke et al., 2000; Louda et al., 2008), which are formed as a result of detoxification catabolism of chloropigments during herbivory (Kashiyama et al., 2012). An abundance of BiCAPs in the sulfur-bound fraction is in contrast to the non-sulfur-bound fraction dominated by cycloalkanoporphyrins (Keely et al., 1995), and has, similarly, been observed in the Gibellina marls (Sicily, Italy) deposited during the MSC (Schaeffer et al., 1993, 1994). The preservation efficiency of BiCAP-type porphyrins may have been enhanced due to their incorporation into macromolecular entities *via* sulfur binding during the early stage of diagenesis, resulting in survival during subsequent diagenetic processes.

The second abundant was deoxophylloerythroetioporphyrin (DPEP, 4a), which is generally the most abundant porphyrin type in geological samples. The DPEP and C_{30}-3-methyl-13-nor-phylloporphyrin (1a), which is considered to be derived from the opening of a five-membered ring between the C-13 and C-15 carbons of DPEP (Callot and Ocampo, 2000), are categorized as DPEP-type. They are derived from multiple sources including chlorophyll *a*, chlorophyll *c*, and bacteriochlorophyll *a* (Baker and Louda, 1986; Callot and Ocampo, 2000; Keely, 2006).

The third abundant C_{31}-15,17-methylcyclopentanoporphyrin (3a) is more source-specific, believed to be originating exclusively from chlorophyll *c* (Ocampo et al., 1984). Together with C_{29}-3-methyl-17-nor-DPEP (1b) which also derive from chlorophyll *c* (Verne-Mismer et al., 1988), these geoporphyrins strongly suggest the presence of chlorophyll *c*-producing eukaryotic algae. Although chlorophyll *a* is more abundant than chlorophyll *c* in living diatoms (Stauber and Jeffrey, 1988) and dinoflagellates (Jeffrey et al., 1975), the Chl *c*-type porphyrins were as abundant as the DPEP-type which potentially derived from not only

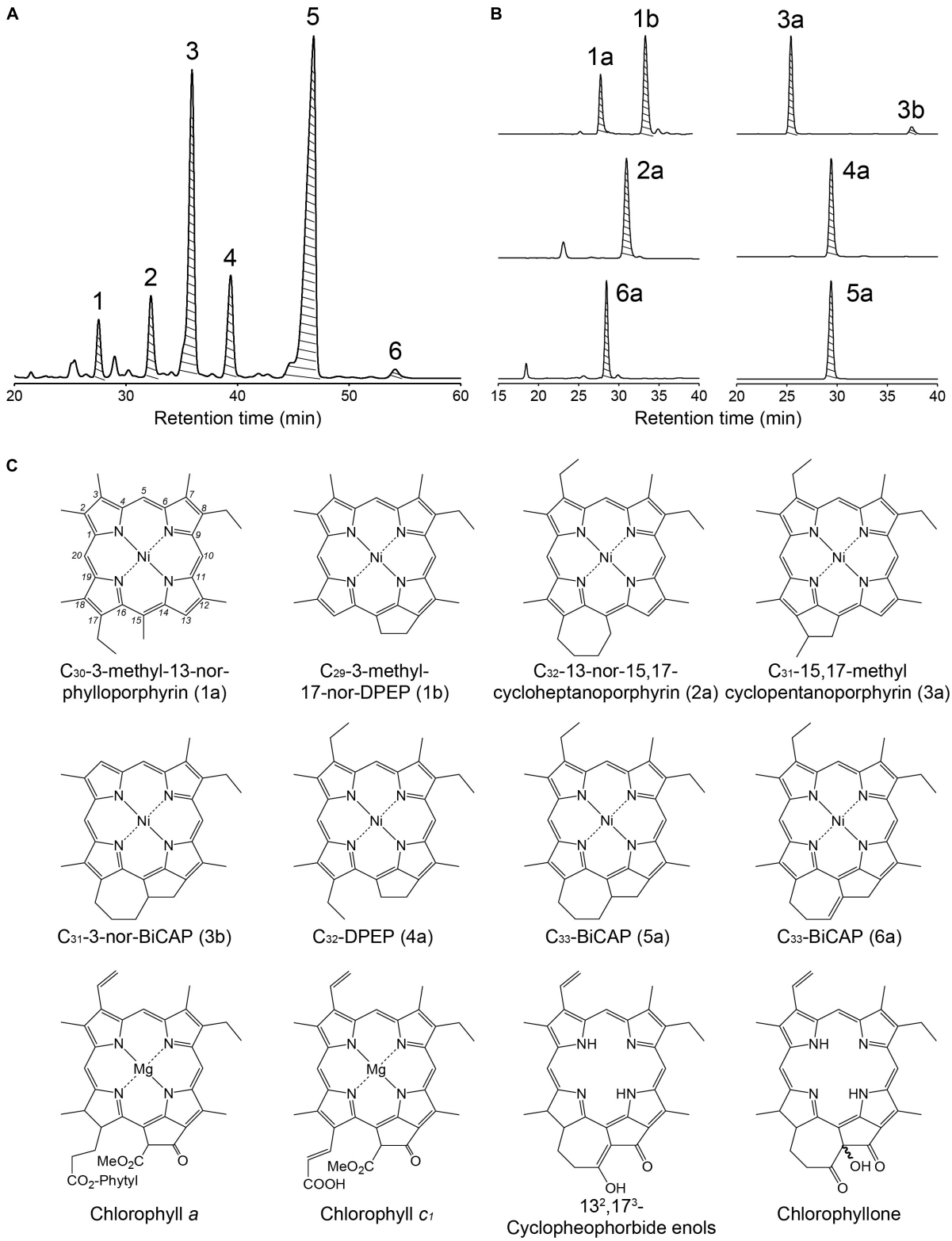

FIGURE 2 | (A) Chromatogram of the first-step, reverse-phase HPLC/DAD at 386 nm of the Ni alkylporphyrins fraction from the PLG 4 shale. Shaded peaks indicate the fraction collected for further purification using a normal-phase HPLC. **(B)** Chromatogram of the second-step, normal-phase HPLC/DAD at 386 nm of the peaks 1–6 collected in a reverse-phase step. Shaded peaks were fraction collected for measurements of carbon and nitrogen isotopic compositions and for determining the structures of porphyrins. **(C)** Structures of geoporphyrins and related compounds discussed in this study. Compounds 1a, 1b, 3b, and 6a are tentatively assigned.

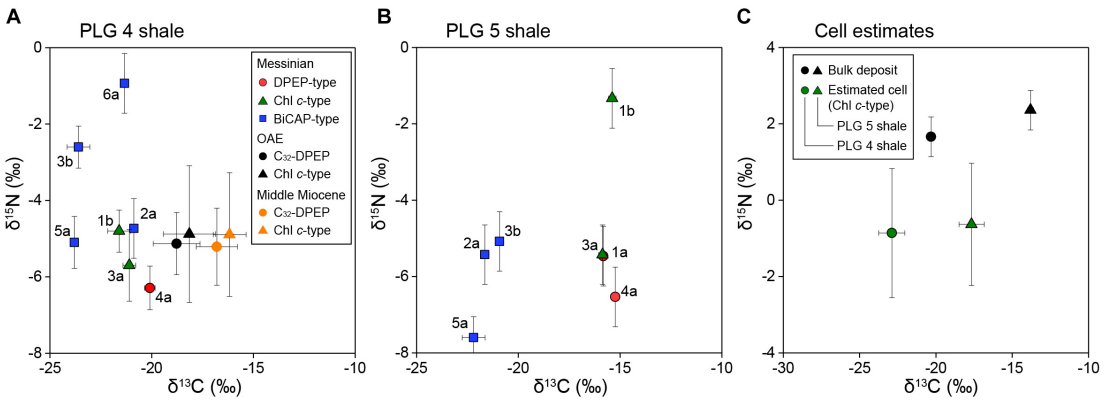

FIGURE 3 | (A,B) Cross plots of the carbon and nitrogen isotopic compositions of purified alkylporphyrins from the PLG shales. The DPEP-type porphyrins are shown by red circles, the Chl *c*-type by green triangles, and the BiCAP-type by blue squares. Letters next to the symbols refer to the individual porphyrins in **Figure 2**. The bars of each symbols represent analytical precisions. Also shown are the isotopic compositions of DPEP and C_{30}-17-nor-DPEP (Chl *c*-type) from the black shales of the Cretaceous Oceanic Anoxic Event and the Miocene siliceous sediments of the eastern margin of the Japan Sea (Kashiyama et al., 2008a,b, 2010). The bars of each symbols represent the range of variation among different samples. **(C)** Cross plots of the carbon and nitrogen isotopic compositions of the bulk deposits and the source phototrophic cells of compound 3a (Chl *c*-type), assuming the porphyrins are enriched in ^{13}C by 1.8 ± 0.8‰ (1σ, *n* = 18) and depleted in ^{15}N by 4.8 ± 1.4‰ (1σ, *n* = 20) relative to the source phototrophs (Sachs et al., 1999; Ohkouchi et al., 2006, 2008).

TABLE 1 | Molecular ion (*m/z*), number of carbons, theoretical C/N weight ratio, measured C/N weight ratio, $\delta^{13}C$, and $\delta^{15}N$ of the bulk sediments and geoporphyrins of the PLG shales in Vena del Gesso, Northern Apennines, Italy.

Compound	Molecular Ion (*m/z*)	Theoretical C/N wt	PLG 4 shale			PLG 5 shale		
			Measured C/N wt	$\delta^{13}C$ (‰)	$\delta^{15}N$ (‰)	Measured C/N wt	$\delta^{13}C$ (‰)	$\delta^{15}N$ (‰)
Bulk deposit			24.3	−20.3	1.7	34.8	−13.8	2.4
1a	506	6.4				7.9	−15.8	−5.5
1b	490	6.2	7.7	−21.6	−4.8	6.6	−15.4	−1.3
2a	532	6.9	7.2	−20.9	−4.7	7.0	−21.6	−5.4
3a	518	6.6	6.8	−21.1	−5.7	7.1	−15.9	−5.4
3b	516	6.6	7.9	−23.6	−2.6	7.6	−20.9	−5.1
4a	532	6.9	7.3	−20.1	−6.3	7.0	−15.2	−6.5
5a	544	7.1	7.4	−23.8	−5.1	7.5	−22.2	−7.6
6a	542	7.1	7.1	−21.3	−0.9			

Names of the compounds refer to individual porphyrins indicated in ***Figure 2****. The analytical precisions for the porphyrin isotopic measurements were within ±0.3‰ for* $\delta^{13}C$ *and ±0.8‰ for* $\delta^{15}N$.

chlorophyll *c* but also chlorophyll *a*. This can be explained by examining the process by which the tetrapyrrole nucleus of chlorophylls *a* and *c* are formed: whereas chlorophyll *a* has a chlorin-ring requiring the aromatization step to form porphyrin, chlorophyll *c* originally has a porphyrin-ring and does not require this step. Indeed, chlorins were detected in the PLG shales (Keely et al., 1995; Mawson and Keely, 2008), suggesting that the conversion of the chlorin-ring chloropigments to alkylporphyrin has not completed.

Stable Isotopic Compositions of Bulk Sediments and Geoporphyrins

The stable carbon isotopic composition of total organic carbon ($\delta^{13}C_{TOC}$) of PLG 4 was much lower than that of PLG 5 (−20.3 and −13.8‰, respectively), and their $\delta^{15}N$ values were similar (1.7 and 2.4‰, respectively; **Figures 3A,B** and **Table 1**). Their C/N weight ratios were as high as 24.3 and 34.8, respectively, a phenomenon that has been often observed in organic-rich sediments (Ohkouchi et al., 2015). The $\delta^{13}C$ values of the individual geoporphyrins showed similar bimodal distributions in the two shales, with a BiCAP-type lower than DPEP-type and Chl *c*-type. The difference was larger in PLG 5, due to higher $\delta^{13}C$ values of the Chl *c*-type in PLG 5 relative to those in PLG 4. The $\delta^{15}N$ values of the geoporphyrins of the two shales varied widely between −7.6 and −0.9‰, but the major porphyrins (2a, 3a, 4a, and 5a) showed a narrower isotopic range from −7.6 to −4.7‰.

DISCUSSION

Primary Producers and Nitrogen Cycle During the Deposition of the PLG Shales

The PLG shales contain considerable amount of terrigenous organic matter (Sinninghe Damsté et al., 1995). The marine

$\delta^{13}C$ and $\delta^{15}N$ signals are thus superimposed by the isotopic signatures of terrestrial organic matter, and are also potentially altered by diagenesis in the sediments (Lehmann et al., 2002; Robinson et al., 2012). Under such situation, $\delta^{13}C$ and $\delta^{15}N$ values of geoporphyrins are powerful tools providing the original isotopic signatures of marine phototrophs, because the turnover rate of aquatic chlorophylls are substantially faster than that of terrestrial chlorophylls (Hendry et al., 1987), and the terrestrial chloropigments are readily decomposed before reaching to the ocean (Hoyt, 1966; Sanger, 1988; Matile et al., 1996). Also, the Mg-loss during diagenesis does not discriminate nitrogen isotope (Ohkouchi et al., 2005), and Ni-chelation associates little nitrogen isotopic fractionation (Kashiyama et al., 2007), in contrast to the cases for VO- and Zn-porphyrins (Junium et al., 2015).

The empirical $\delta^{13}C$ and $\delta^{15}N$ relationships known between chloropigments and phototrophs enable us to estimate the isotopic compositions of the source phototrophs from geoporphyrins. The $\delta^{13}C$ values of geoporphyrins is 1.8 ± 0.8‰ (1σ, $n = 18$) enriched in ^{13}C relative to the phototrophic cell (Ohkouchi et al., 2008). On the other hand, while the $\delta^{15}N$ values of chloropigments is 4.8 ± 1.4‰ (1σ, $n = 20$) depleted in ^{15}N relative to the cell of eukaryotic algae and purple sulfur bacteria (Sachs et al., 1999; Ohkouchi et al., 2006; Higgins et al., 2011), several different relationships have been reported for the $\delta^{15}N$ values of chlorophyll *a* and cyanobacteria: ^{15}N enrichment of ∼10‰ (Beaumont et al., 2000; Higgins et al., 2011), ^{15}N depletion of ∼1‰ (Higgins et al., 2011), or ^{15}N depletion of ∼5‰ (Sachs et al., 1999) in chlorophyll *a* relative to the cell. These complex relationships of cyanobacteria complicate the estimation of the $\delta^{15}N$ values of past phototrophic biomass from geoporphyrins.

Thus, our discussion here is primarily based on the isotopic compositions of Chl *c*-type porphyrins, which provide us with robust isotopic estimates of chlorophyll *c*-producing eukaryotic phototrophs. Their $\delta^{13}C$ values calculated from the representative Chl *c*-type porphyrin (compound 3a) are -22.9 ± 0.9 and -17.7 ± 0.8‰ (1σ), and $\delta^{15}N$ values -0.9 ± 1.7 and -0.6 ± 1.6‰ (1σ) for PLG 4 and 5 shales, respectively (**Figure 3C**). This $\delta^{13}C$ value of the PLG 4 shale was in comparable range with those of C_{25} highly-branched isoprenoids (−23.9 and −27.3‰) derived from diatoms and dinosterane (−26.3‰) from dinoflagellates (**Supplementary Figure S6**; Kohnen et al., 1992; Kenig et al., 1995), considering that the lipids are depleted in ^{13}C relative to the eukaryotic cell (Schouten et al., 1998; Hayes, 2001). These chlorophyll *c*-producing algae are the major components of the marine organic matter in the sediments, as the ∼6‰ difference in $\delta^{13}C_{TOC}$ between PLG 4 and 5 shales was associated with similar shift in $\delta^{13}C$ of the Chl *c*-type porphyrins (**Figure 3C**).

Relatively high $\delta^{13}C$ of chlorophyll *c*-producing algae in part explains the ^{13}C-enrichment in TOC of the PLG shales compared to other stratified basins (e.g., van Breugel et al., 2005). In addition, considering that other MSC deposits also exhibit elevated $\delta^{13}C_{TOC}$ (Schouten et al., 2001; Yoshimura et al., 2016), a physicochemical process specific to hypersaline condition, such as the degassing of ^{13}C-depleted CO_2(aq) from the brine induced by a decrease in gas solubility during evaporation (Stiller et al., 1985; Isaji et al., 2017), may also have contributed to $\delta^{13}C_{TOC}$ increase. It is noteworthy that, compared to other modern and ancient stratified basins, the $\delta^{13}C$ values of the CO_2 at the chemocline during the deposition of PLG 4 shale are less depleted in ^{13}C with respect to CO_2(atm) (van Breugel et al., 2005). Such a ^{13}C-enrichment at the chemocline, especially at the onset of the shale deposition ($\delta^{13}C$ = ∼8%; van Breugel et al., 2005), may in part have been the result of the degassing of ^{13}C-depleted CO_2(aq) from the brine during the gypsum-precipitating phase prior to the shale deposition.

The $\delta^{15}N$ values of these chlorophyll *c*-producing algae fall within a range typical for diazotrophy (−2–0‰: Wada, 1980). Since breaking the triple bond of N_2 is energetically expensive, N_2-fixation is generally successful where nitrate and ammonium are limited relative to phosphate. During the deposition of the PLG shales, the continental water inflow formed strong density stratification and produced photic zone anoxia (Sinninghe Damsté et al., 1995; Lugli et al., 2010). Thus, the supply of nutrients from the bottom layer must have been reduced, and the N/P ratio of the supplied nutrients lowered by denitrification and/or anammox in the redox boundary. Indeed, similar processes have been considered to have promoted N_2-fixation by cyanobacteria in the Black Sea (Kuypers et al., 2003; Kusch et al., 2010; Fulton et al., 2012), which is a restricted, stratified-basin analogous to the depositional environment of the Vena del Gesso basin. Alternative explanations for relatively low $\delta^{15}N$ values of phototrophs, such as excess nitrate resulting in large isotopic fractionation during nitrate assimilation or low $\delta^{15}N$ of the original nitrate, are unlikely, because denitrification decreases the N/P ratio and increases the $\delta^{15}N$ of the remaining nitrate (Brandes et al., 1998).

Assimilation of ammonium supplied from the subsurface could also explain ^{15}N-depleted biomass, because the nitrogen isotopic fractionation associated with ammonium assimilation can be large, ranging from −4 to −20‰ (Hoch et al., 1992; Liu et al., 2013). Importance of ammonium as a nitrogen source under stratified condition has indeed been implicated from the sedimentary records of the Black Sea and a shallow lake Baldeggersee (Teranes and Bernasconi, 2000; Kusch et al., 2010). Although much stronger density stratification formed in the Vena del Gesso basin should have resulted in slower ammonium supply rate compared to these modern analogs, the possibility of ammonium assimilation cannot be eliminated as we have no constraints on the depth of chemocline during the deposition of the PLG shales. It is noteworthy, however, that assimilation of subsurface ammonium by phototrophs during the MSC peak resulted in extremely elevated $\delta^{15}N$ of geoporphyrins (Isaji et al., 2019), which highly contrasts with the results in this study (discussed in Section "Fluctuations in the Chemocline Depth Associating Shifts in the Nitrogen Cycle").

Because N_2-fixation is an exclusively prokaryotic metabolic process, the $\delta^{15}N$ values of the chlorophyll *c*-producing algae indicating diazotrophy need specific explanation. Here, we suggest that the algae assimilated nitrogen fixed originally by

diazotrophs. For example, complete assimilation of ammonium produced by remineralization of diazotrophs in the photic zone where nitrification is inhibited (Guerrero and Jones, 1996) would result in $\delta^{15}N$ of eukaryotic algae in the range indicative of N_2-fixation. Alternatively, diazotrophic cyanobacteria may have formed symbiosis between diatoms (diatom–diazotrophic associations, DDAs). Diatoms are typically adapted to eutrophic waters, but DDAs can thrive under nitrate-depleted conditions, benefiting from the supply of nitrogen through the N_2-fixation of cyanobacteria symbionts. Several diatom species including some *Rhizosolenia* sp. known to form DDAs (Foster and O'Mullan, 2008) may have been the source of highly-branched isoprenoids preserved in the PLG shales (Sinninghe Damsté et al., 1995), although highly-branched isoprenoids of DDA-forming species have not been investigated.

An important difference between free-living cyanobacteria and DDAs is that while the former are mostly recycled in the upper water column, the latter are reported to contribute substantially to export production (Scharek et al., 1999; Subramaniam et al., 2008; Karl et al., 2012). Such preferential exportation of DDAs may explain the predominance of chlorophyll *c*-producing algae as the main components of the organic matter in the PLG shales. It is noteworthy that abundant Rhizosolenid diatoms and *Hemiaulus hauckii* are considered to have formed DDAs during the deposition of the Mediterranean organic-rich sapropels, which are, similarly, deposited under stratified condition (Kemp et al., 1999; Sachs and Repeta, 1999; Bauersachs et al., 2010; Kemp and Villareal, 2013). The significance of DDAs has also been implied in other organic-rich deposits, such as the black shales of the Cretaceous Oceanic Anoxic Events and the Miocene siliceous sediments in the eastern margin of the Japan Sea, which show surprisingly similar $\delta^{13}C$ and $\delta^{15}N$ profiles to the geoporphyrins from our study (**Figure 3A**; Kashiyama et al., 2008a,b, 2010; Ohkouchi et al., 2015). Also, it should be emphasized that the $\delta^{15}N$ values of most of the geoporphyrins purified from other organic-rich shales deposited under stratified condition falls within similar range as found in this study (**Figure 4**). Taken together, our results and these previous studies indicate the importance of diazotrophy in forming the organic-rich sediments that occur under stratified conditions, in particular DDAs which contribute substantially to efficient carbon sequestration.

Other alkylporphyrins are less source-specific, but still provide additional insights. The $\delta^{13}C$ and $\delta^{15}N$ values of the DPEP-type were similar to those of the Chl *c*-type porphyrins (**Figures 3A,B**), which is probably due to faster conversion of chlorophyll *c* to DPEP relative to other chlorin-ring chloropigments such as chlorophyll *a* and bacteriochlorophyll *a*. The enrichment in ^{13}C by $\sim$1‰ in the DPEP-type relative to the Chl *c*-type may reflect that these chlorin-ring chloropigments had higher $\delta^{13}C$ values compared to chlorophyll *c*. If this was the case, then the major source of DPEP would probably be chlorophyll *a*, because $\delta^{13}C$ of bacteriochlorophyll *a* is typically lower than other co-occurring chloropigments in the modern stratified environments (Ohkouchi et al., 2005; Fulton et al., 2018). In the case of the immature sediments, the isotopic compositions of the chlorins may provide further insights of past phototrophic activities.

Among the BiCAP-type porphyrins, the most abundant C_{33}-BiCAP (compound 5a) was depleted in ^{13}C relative to the Chl *c*-type porphyrins by 2.7 and 6.3‰ for the PLG 4 and 5 shales, respectively (**Figures 3A,B**). These results indicate that C_{33}-BiCAP was derived from specific phototrophs rather than from the major primary producers producing DPEP-type or Chl *c*-type porphyrins. The substantial ^{13}C-depletion may be related with difference in carbon assimilation pathway of phototrophs, and/or difference in $\delta^{13}C$ of source DIC which has depth and seasonal variabilities. Although specific source cannot be identified, brown-colored green sulfur bacteria can at least be excluded as the possible source of BiCAP-type porphyrins, because the $\delta^{13}C$ values of isorenieratane, which has similar $\delta^{13}C$ values to that of bacteriochlorophyll *e* (Ohkouchi et al.,

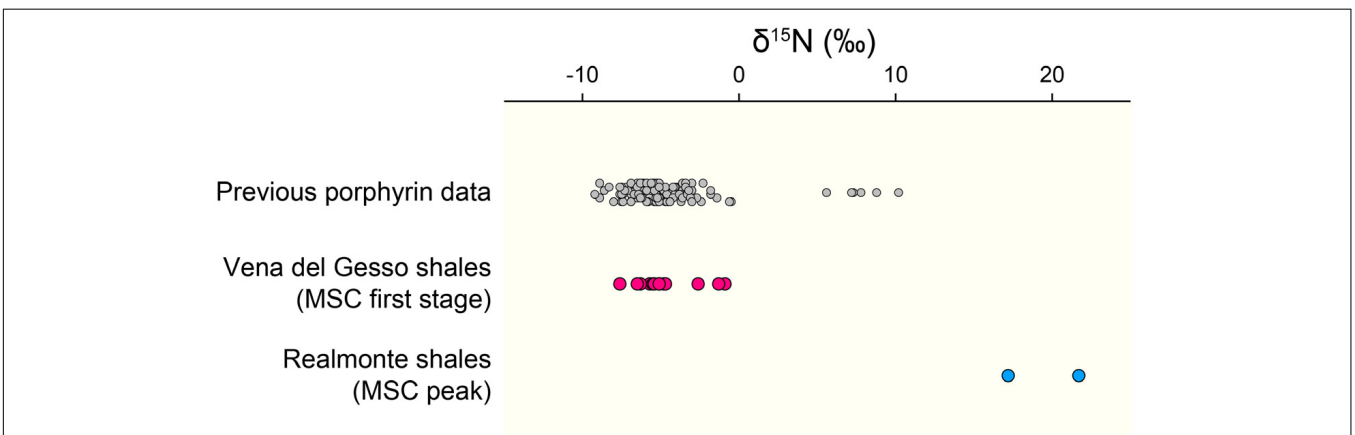

FIGURE 4 | The $\delta^{15}N$ values of geoporphyrins compiled from previous studies (gray circles: Chicarelli et al., 1993; Ohkouchi et al., 2006; Kashiyama et al., 2008a,b, 2010; Higgins et al., 2012; Junium et al., 2015; Gueneli et al., 2018), those determined for the PLG shales in this study (pink circles), and those of the shale layers in the Realmonte salt mine in Sicily deposited during the MSC peak (blue circles: Isaji et al., 2019).

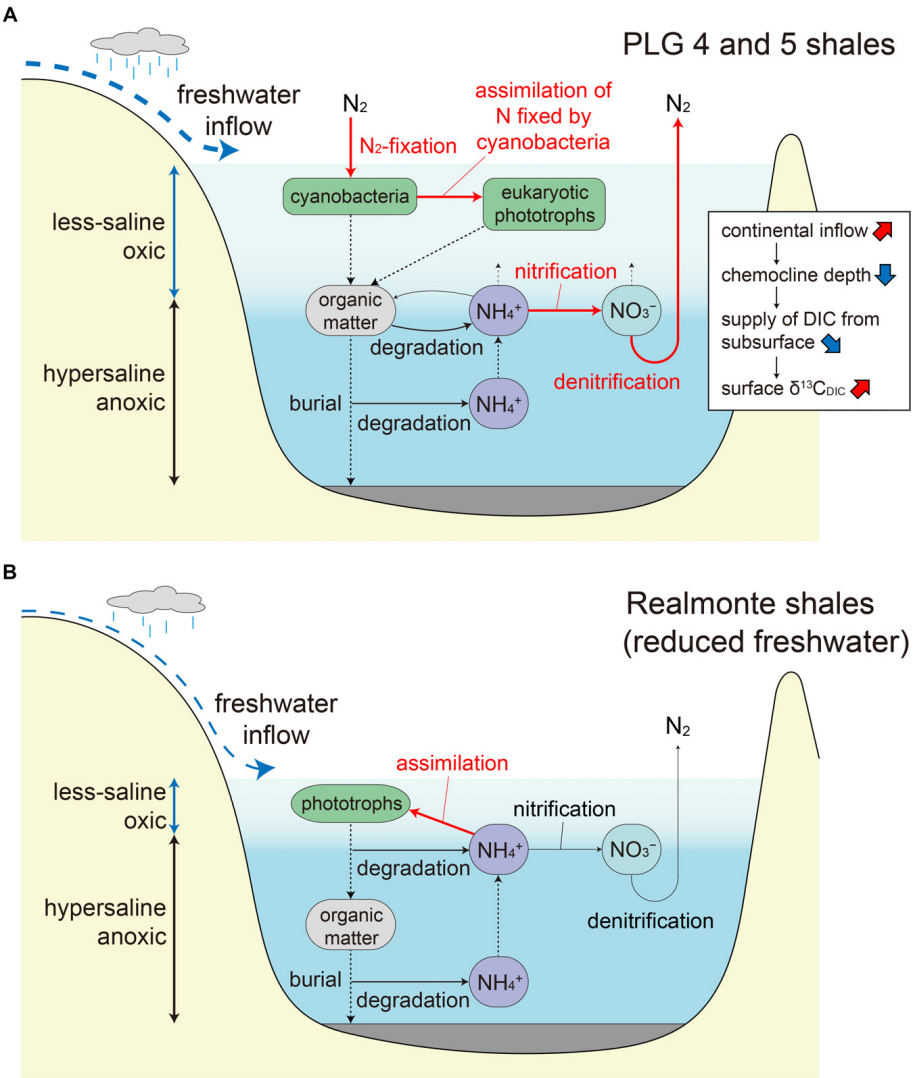

FIGURE 5 | (A) Proposed nitrogen cycle during the deposition of the PLG 4 and 5 shales. Water column stratification resulted in active denitrification (and/or anammox) and limited nitrogen supply to the surface photic zone, resulting in surface water oligotrophy favorable for diazotrophic cyanobacteria. The surface freshwater layer is thicker and the chemocline is deeper during the deposition of the PLG 5 shale due to an increase in regional precipitation, which resulted in a reduced supply of ^{13}C-depleted dissolved inorganic carbon from the bottom hypersaline layer. Important processes are indicated by red arrows. **(B)** Proposed nitrogen cycle under reduced freshwater input during the MSC peak (Isaji et al., 2019). The shallow chemocline results in phototrophic assimilation of the subsurface ammonium rather than nitrification followed by denitrification (and/or anammox).

2005), vary between −14.8 and −11.6‰ in the PLG 4 shale (Kenig et al., 1995).

Fluctuations in the Chemocline Depth Associating Shifts in the Nitrogen Cycle

The isotopic compositions of geoporphyrins clearly demonstrate that 6.5‰ difference in $\delta^{13}C_{TOC}$ between the two shales is not attributable to diagenetic alteration or contribution of terrestrial organic matter, but is associated with changes in $\delta^{13}C$ of marine phototrophs, which is reflected as 5.2‰ difference in the $\delta^{13}C$ of Chl *c*-type porphyrin (**Figure 3**). Phototrophic community composition is not responsible for the $\delta^{13}C$ shift, as the structural distribution of sulfur-bound Ni alkylporphyrin and their $\delta^{15}N$ signatures of the two shales were similar (**Figure 3** and **Supplementary Figure S1**).

This substantial $\delta^{13}C$ difference probably reflects difference in the depositional environment of PLG 4 and PLG 5, rather than intra-layer variation which ranges within $\delta^{13}C_{TOC}$ of ∼2‰ in the middle part of the shale layers where our samples were collected (Kenig et al., 1995). A previous study on pollen assemblages suggested enhanced river discharge during the deposition of the PLG 5 shale compared to that during the PLG 4 (Bertini, 2006). Such hydrologic difference may have modified $\delta^{13}C$ of dissolved inorganic carbon ($\delta^{13}C_{DIC}$) in the surface ocean through varying mixing rate of river water, and altering the $\delta^{13}C$ of riverine

DIC associated with shift in the drainage area. It may also have changed the duration of the stratification vs. vertical mixing periods within each shale layer, with longer duration of mixing period resulting in enhanced supply of ^{13}C-depleted DIC from subsurface water, although the organic geochemical signals are generally not well preserved where oxic condition prevails. More likely, $\delta^{13}C_{DIC}$ in the surface ocean must have been strongly influenced by the depth of chemocline, which changes in response to the amount of river discharge. The elevated δ^{13}C in PLG 5 relative to PLG 4 may have been the result of reduced supply of ^{13}C-depleted DIC from subsurface water due to deeper chemocline depth (**Figure 5A**).

The PLG shales analyzed in this study were deposited when the chemocline was deep enough to induce nitrification–denitrification (and/or anammox) coupling and a predominance of diazotrophic cyanobacteria, which is recorded as a specific δ^{15}N range between −7 and −5‰. Significantly, substantial elevation in δ^{15}N values (≈20‰) are recorded in the geoporphyrins isolated from the mud–anhydrite layers deposited under density-stratified condition during the MSC peak (**Figure 4**; Isaji et al., 2019). This contrasting signal is interpreted to reflect the assimilation of ^{15}N-enriched ammonium pools from the subsurface and the recycling of bioavailable nitrogen within the water column with shallow chemocline (**Figure 5B**). The dynamic shifts in the mode of the nitrogen cycle under density-stratified condition must have resulted in modification of the phototrophic community and the primary productivity, which associate changes in the strength of the biological pump controlling the global carbon cycle.

CONCLUSION

Major primary producers and the nitrogen cycle during the deposition of the PLG shales of the MSC were discussed, based on the analyses on geoporphyrins which possess unaltered record of stable carbon and nitrogen isotopic compositions of marine phototrophs in the geologic past. Reduced nutrient supply and lowering of N/P ratio under density-stratified conditions favored diazotrophs which supplied a major fraction of the nitrogen for the total photoautotrophic community, possibly in particular as symbionts of diatoms characterized by high export production. The substantially higher δ^{13}C values of TOC, DPEP-type, and Chl *c*-type porphyrins in the PLG 5 shale compared with those in the PLG 4 were attributed to a lower supply of ^{13}C-depleted DIC from the bottom water to the photic zone as a result of deepening of the chemocline. We suggest that the mode of the nitrogen cycle shifted dynamically (nitrification–denitrification–N_2-fixation coupling vs. phototrophic assimilation of ammonium) by changing the depth of the chemocline under density-stratified condition during the MSC.

AUTHOR CONTRIBUTIONS

YI, HK, JK, TY, and NO designed the study. SL, VM, and MR collected the samples. YI, YT, and NOO conducted the experimental work and data analysis. YI and NO wrote the manuscript. All the authors edited and revised the manuscript.

FUNDING

This study was partly supported by a Japan Society for the Promotion of Science (JSPS) Research Fellowship (16J07844) to YI, a Grants-in-Aid (16H02236), and the JAMSTEC President Fund to NO.

ACKNOWLEDGMENTS

We acknowledge H. Suga for assistance in the laboratory works, and A. Toki and K. Ishikawa for help with sample preparation. We thank F. J. Jiménez-Espejo for helpful discussions.

SUPPLEMENTARY MATERIAL

The Supplementary Material for this article can be found online at: https://www.frontiersin.org/articles/10.3389/feart.2019.00085/full#supplementary-material

REFERENCES

Baker, E. W., and Louda, J. W. (1986). "Porphyrins in the geological record," in *Biological Markers in Sediments. Methods in Geochemistry and Geophysics*, Vol. 24, ed. R. B. Johns (Amsterdam: Elsevier), 125–225.

Bauersachs, T., Speelman, E. N., Hopmans, E. C., Reichart, G.-J., Schouten, S., and Sinninghe Damsté, J. S. (2010). Fossilized glycolipids reveal past oceanic N2 fixation by heterocystous cyanobacteria. *Proc. Natl. Acad. Sci. U.S.A.* 107, 19190–19194. doi: 10.1073/pnas.1007526107

Beaumont, V. I., Jahnke, L. L., and Des Marais, D. J. (2000). Nitrogen isotopic fractionation in the synthesis of photosynthetic pigments in *Rhodobacter capsulatus* and *Anabaena cylindrica*. *Org. Geochem.* 31, 1075–1085. doi: 10.1016/s0146-6380(00)00133-9

Berger, W. H., Smetacek, V. S., and Wefer, G. (1989). *Productivity of the Ocean: Present and Past*. New York, NY: Wiley-Interscience, 470.

Bertini, A. (2006). The northern apennines palynological record as a contribute for the reconstruction of the Messinian palaeoenvironments. *Sediment. Geol.* 188, 235–258. doi: 10.1016/j.sedgeo.2006.03.007

Boreham, C. J., Fookes, C. J., Popp, B. N., and Hayes, J. (1989). Origins of etioporphyrins in sediments: evidence from stable carbon isotopes. *Geochim. Cosmochim. Acta* 53, 2451–2455. doi: 10.1016/0016-7037(89)90368-2

Boreham, C. J., Fookes, C. J., Popp, B. N., and Hayes, J. (1990). Origin of petroporphyrins. 2. Evidence from stable carbon isotopes. *Energy Fuels* 4, 658–661. doi: 10.1021/ef00024a007

Brandes, J. A., Devol, A. H., and Deutsch, C. (2007). New developments in the marine nitrogen cycle. *Chem. Rev.* 107, 577–589. doi: 10.1021/cr050377t

Brandes, J. A., Devol, A. H., Yoshinari, T., Jayakumar, D., and Naqvi, S. (1998). Isotopic composition of nitrate in the central Arabian Sea and eastern tropical North Pacific: a tracer for mixing and nitrogen cycles. *Limnol. Oceanogr.* 43, 1680–1689. doi: 10.4319/lo.1998.43.7.1680

Callot, H. J., and Ocampo, R. (2000). "Geochemistry of porphyrins," in *The Porphyrin Handbook, Synthetic and Organic Chemistry*, Vol. 1, eds K. M. Kadish, K. M. Smith, and R. Guiland (New York, NY: Academic Press), 349–398.

Chicarelli, M. I., Hayes, J., Popp, B. N., Eckardt, C. B., and Maxwell, J. R. (1993). Carbon and nitrogen isotopic compositions of alkyl porphyrins from

the Triassic Serpiano oil shale. *Geochim. Cosmochim. Acta* 57, 1307–1311. doi: 10.1016/0016-7037(93)90067-7

Foster, R., and O'Mullan, G. (2008). "Nitrogen-fixing and nitrifying symbioses in the marine environment," in *Nitrogen in the Marine Environment*, eds D. G. Capone, D. A. Bronk, M. R. Mulholland, and E. J. Carpenter (New York, NY: Academic Press), 1197–1218. doi: 10.1016/b978-0-12-372522-6.00027-x

Fulton, J., Arthur, M., Thomas, B., and Freeman, K. (2018). Pigment carbon and nitrogen isotopic signatures in euxinic basins. *Geobiology* 16, 429–445. doi: 10.1111/gbi.12285

Fulton, J. M., Arthur, M. A., and Freeman, K. H. (2012). Black sea nitrogen cycling and the preservation of phytoplankton δ15N signals during the Holocene. *Glob. Biogeochem. Cycles* 26:GB2030.

Goericke, R., Strom, S. L., and Bell, M. A. (2000). Distribution and sources of cyclic pheophorbides in the marine environment. *Limnol. Oceanogr.* 45, 200–211. doi: 10.4319/lo.2000.45.1.0200

Gueneli, N., McKenna, A. M., Ohkouchi, N., Boreham, C. J., Beghin, J., Javaux, E. J., et al. (2018). 1.1-billion-year-old porphyrins establish a marine ecosystem dominated by bacterial primary producers. *Proc. Natl. Acad. Sci. U.S.A.* 115, E6978–E6986. doi: 10.1073/pnas.1803866115

Guerrero, M. A., and Jones, R. D. (1996). Photoinhibition of marine nitrifying bacteria. I. Wavelength-dependent response. *Mar. Ecol. Prog. Ser.* 141, 183–192. doi: 10.3354/meps141183

Hay, W. W., Migdisov, A., Balukhovsky, A. N., Wold, C. N., Flögel, S., and Söding, E. (2006). Evaporites and the salinity of the ocean during the Phanerozoic: implications for climate, ocean circulation and life. *Palaeogeogr. Palaeoclimatol. Palaeoecol.* 240, 3–46. doi: 10.1016/j.palaeo.2006.03.044

Hayes, J., Takigiku, R., Ocampo, R., Callot, H. J., and Albrecht, P. (1987). Isotopic compositions and probable origins of organic molecules in the eocene messel shale. *Nature* 329, 48–51. doi: 10.1038/329048a0

Hayes, J. M. (2001). Fractionation of carbon and hydrogen isotopes in biosynthetic processes. *Rev. Mineral Geochem.* 43, 225–277. doi: 10.2138/gsrmg.43.1.225

Hendry, G. A., Houghton, J. D., and Brown, S. B. (1987). The degradation of chlorophyll—a biological enigma. *New Phytol.* 107, 255–302. doi: 10.1111/j.1469-8137.1987.tb00181.x

Higgins, M. B., Robinson, R. S., Husson, J. M., Carter, S. J., and Pearson, A. (2012). Dominant eukaryotic export production during ocean anoxic events reflects the importance of recycled NH4+. *Proc. Natl. Acad. Sci. U.S.A.* 109, 2269–2274. doi: 10.1073/pnas.1104313109

Higgins, M. B., Wolfe-Simon, F., Robinson, R. S., Qin, Y., Saito, M. A., and Pearson, A. (2011). Paleoenvironmental implications of taxonomic variation among δ15N values of chloropigments. *Geochim. Cosmochim. Acta* 75, 7351–7363. doi: 10.1016/j.gca.2011.04.024

Hoch, M. P., Fogel, M. L., and Kirchman, D. L. (1992). Isotope fractionation associated with ammonium uptake by a marine bacterium. *Limnol. Ocreanogr.* 37, 1447–1459. doi: 10.4319/lo.1992.37.7.1447

Honjo, S., Manganini, S. J., Krishfield, R. A., and Francois, R. (2008). Particulate organic carbon fluxes to the ocean interior and factors controlling the biological pump: a synthesis of global sediment trap programs since 1983. *Prog. Oceanogr.* 76, 217–285. doi: 10.1016/j.pocean.2007.11.003

Hoyt, P. B. (1966). Chlorophyll-type compounds in soil. *Plant Soil* 25, 313–328. doi: 10.1007/bf01394456

Hsü, K., Ryan, W., and Cita, M. (1973). Late miocene desiccation of the mediterranean. *Nature* 242, 240–244. doi: 10.1038/242240a0

Isaji, Y., Kawahata, H., Kuroda, J., Yoshimura, T., Ogawa, N. O., Suzuki, A., et al. (2017). Biological and physical modification of carbonate system parameters along the salinity gradient in shallow hypersaline solar salterns in Trapani, Italy. *Geochim. Cosmochim. Acta* 208, 354–367. doi: 10.1016/j.gca.2017.04.013

Isaji, Y., Kawahata, H., Ogawa, N. O., Kuroda, J., Yoshimura, T., Jiménez-Espejo, F. J., et al. (2019). Efficient recycling of nutrients in modern and past hypersaline environments. *Sci. Rep.* 9:3718. doi: 10.1038/s41598-019-40174-9

Jeffrey, S., Sielicki, M., and Haxo, F. T. (1975). Chloroplast pigment patterns in dinoflagellates. *J. Phycol.* 11, 374–384. doi: 10.1111/j.1529-8817.1975.tb02799.x

Junium, C. K., Freeman, K. H., and Arthur, M. A. (2015). Controls on the stratigraphic distribution and nitrogen isotopic composition of zinc, vanadyl and free base porphyrins through oceanic anoxic event 2 at demerara rise. *Org. Geochem.* 80, 60–71. doi: 10.1016/j.orggeochem.2014.10.009

Karl, D. M., Church, M. J., Dore, J. E., Letelier, R. M., and Mahaffey, C. (2012). Predictable and efficient carbon sequestration in the North Pacific Ocean supported by symbiotic nitrogen fixation. *Proc. Natl. Acad. Sci. U.S.A.* 109, 1842–1849. doi: 10.1073/pnas.1120312109

Kashiyama, Y., Kitazato, H., and Ohkouchi, N. (2007). An improved method for isolation and purification of sedimentary porphyrins by high-performance liquid chromatography for compound-specific isotopic analysis. *J. Chromatogr. A* 1138, 73–83. doi: 10.1016/j.chroma.2006.10.028

Kashiyama, Y., Ogawa, N. O., Kuroda, J., Shiro, M., Nomoto, S., Tada, R., et al. (2008a). Diazotrophic cyanobacteria as the major photoautotrophs during mid-Cretaceous oceanic anoxic events: nitrogen and carbon isotopic evidence from sedimentary porphyrin. *Org. Geochem.* 39, 532–549. doi: 10.1016/j.orggeochem.2007.11.010

Kashiyama, Y., Ogawa, N. O., Shiro, M., Tada, R., Kitazato, H., and Ohkouchi, N. (2008b). Reconstruction of the biogeochemistry and ecology of photoautotrophs based on the nitrogen and carbon isotopic compositions of vanadyl porphyrins from Miocene siliceous sediments. *Biogeosciences* 5, 361–409. doi: 10.5194/bgd-5-361-2008

Kashiyama, Y., Ogawa, N. O., Nomoto, S., Kitazato, H., and Ohkouchi, N. (2010). "Nitrogen and carbon isotopic compositions of copper, nickel, and vanadyl porphyrins in Cretaceous black shales," in *Earth, Life, and Isotopes*, eds N. Ohkouchi, I. Tayasu, and K. Koba (Kyoto: Kyoto University Press), 313–335.

Kashiyama, Y., Yokoyama, A., Kinoshita, Y., Shoji, S., Miyashiya, H., Shiratori, T., et al. (2012). Ubiquity and quantitative significance of detoxification catabolism of chlorophyll associated with protistan herbivory. *Proc. Natl. Acad. Sci. U.S.A.* 109, 17328–17335. doi: 10.1073/pnas.1207347109

Keely, B., Blake, S., Schaeffer, P., and Maxwell, J. (1995). Distributions of pigments in the organic matter of marls from the Vena del Gesso evaporitic sequence. *Org. Geochem.* 23, 527–539. doi: 10.1016/0146-6380(95)00046-h

Keely, B., Harris, P., Popp, B., Hayes, J., Meischner, D., and Maxwell, J. (1994). Porphyrin and chlorin distributions in a Late Pliocene lacustrine sediment. *Geochim. Cosmochim. Acta* 58, 3691–3701. doi: 10.1016/0016-7037(94)90159-7

Keely, B. J. (2006). "Geochemistry of chlorophylls," in *Chlorophylls and Bacteriochlorophylls: Biochemistry, Biophysics, Functions and Applications. Advances in Photosynthesis and Respiration*, eds B. Grimm, R. J. Porra, W. Rüdiger, and H. Scheer (Dordrecht: Springer), 535–561. doi: 10.1007/1-4020-4516-6_37

Kemp, A. E., Pearce, R. B., Koizumi, I., Pike, J., and Rance, S. J. (1999). The role of mat- forming diatoms in the formation of Mediterranean sapropels. *Nature* 398, 57–61. doi: 10.1038/18001

Kemp, A. E., and Villareal, T. A. (2013). High diatom production and export in stratified waters–a potential negative feedback to global warming. *Prog. Oceanogr.* 119, 4–23. doi: 10.1016/j.pocean.2013.06.004

Kenig, F., Sinninghe Damsteì, J. S., Frewin, N. L., Hayes, J., and De Leeuw, J. W. (1995). Molecular indicators for palaeoenvironmental change in a Messinian evaporitic sequence (Vena del Gesso, Italy). II: high-resolution variations in abundances and 13C contents of free and sulphur-bound carbon skeletons in a single marl bed. *Org. Geochem.* 23, 485–526. doi: 10.1016/0146-6380(95)00049-k

Kohnen, M. E., Schouten, S., Sinninghe Damsteì, J. S., de Leeuw, J. W., Merritt, D. A., and Hayes, J. (1992). Recognition of paleobiochemicals by a combined molecular sulfur and isotope geochemical approach. *Science* 256, 358–362. doi: 10.1126/science.256.5055.358

Krijgsman, W., Hilgen, F. J., Raffi, I., Sierro, F. J. and Wilson, D. S. (1999). Chronology, causes and progression of the Messinian salinity crisis. Nature 400, 652–655. doi: 10.1038/23231

Kusch, S., Kashiyama, Y., Ogawa, N. O., Altabet, M., Butzin, M., Friedrich, J., et al. (2010). Implications for chloro-and pheopigment synthesis and preservation from combined compound-specific δ13C, δ15N, and Δ14C analysis. *Biogeosciences* 7, 4105–4118. doi: 10.5194/bg-7-4105-2010

Kuypers, M. M., Sliekers, A. O., Lavik, G., Schmid, M., Jørgensen, B. B., Kuenen, J. G., et al. (2003). Anaerobic ammonium oxidation by anammox bacteria in the Black Sea. *Nature* 422, 608–611. doi: 10.1038/nature01472

Lehmann, M. F., Bernasconi, S. M., Barbieri, A., and McKenzie, J. A. (2002). Preservation of organic matter and alteration of its carbon and nitrogen isotope composition during simulated and in situ early sedimentary diagenesis. *Geochim. Cosmochim. Acta* 66, 3573–3584. doi: 10.1016/s0016-7037(02)00968-7

Liu, K. K., Kao, J. S., Chiang, P. K., Gong, C. G., Chang, J., Cheng, S. J., et al. (2013). Concentration dependent nitrogen isotope fractionation during ammonium

uptake by phytoplankton under an algal bloom condition in the Danshuei estuary, northern Taiwan. *Mar. Chem.* 157, 242–252. doi: 10.1016/j.marchem.2013.10.005

Louda, J., Neto, R., Magalhaes, A., and Schneider, V. (2008). Pigment alterations in the brown mussel *Perna perna*. *Comp. Biochem. Physiol. B Biochem. Mol. Biol.* 150, 385–394. doi: 10.1016/j.cbpb.2008.04.008

Lugli, S., Manzi, V., Roveri, M., and Schreiber, B. C. (2010). The primary lower gypsum in the mediterranean: a new facies interpretation for the first stage of the messinian salinity crisis. *Palaeogeogr. Palaeoclimatol. Palaeoecol.* 297, 83–99. doi: 10.1016/j.palaeo.2010.07.017

Manzi, V., Gennari, R., Lugli, S., Roveri, M., Scafetta, N., and Schreiber, B. C. (2012). High-frequency cyclicity in the mediterranean messinian evaporites: evidence for solar-lunar climate forcing. *J. Sed. Res.* 82, 991–1005. doi: 10.2110/jsr.2012.81

Matile, P., Hortensteiner, S., Thomas, H., and Krautler, B. (1996). Chlorophyll breakdown in senescent leaves. *Plant Physiol.* 112, 1403–1409. doi: 10.1104/pp.112.4.1403

Mawson, D. H., and Keely, B. J. (2008). Novel functionalised chlorins in sediments of the Messinian Vena del Gesso evaporitic sequence: evidence for a facile route to reduction for biomarkers. *Org. Geochem.* 39, 203–209. doi: 10.1016/j.orggeochem.2007.10.005

Ocampo, R., Callot, H., Albrecht, P., and Kintzinger, J. (1984). A novel chlorophyll c related petroporphyrin in oil shale. *Tetrahedron Lett.* 25, 2589–2592. doi: 10.1016/s0040-4039(01)81238-7

Ocampo, R., Callot, H., Albrecht, P., Popp, B., Horowitz, M., and Hayes, J. (1989). Different isotope compositions of C32 DPEP and C32 etioporphyrin III in oil shale. *Naturwissenschaften* 76, 419–421. doi: 10.1007/bf00366165

Ogawa, N. O., Nagata, T., Kitazato, H., and Ohkouchi, N. (2010). "Ultra-sensitive elemental analyzer/isotope ratio mass spectrometer for stable nitrogen and carbon isotope analyses," in *Earth, Life, and Isotopes*, eds N. Ohkouchi, I. Tayasu, and K. Koba (Kyoto: Kyoto University Press), 339–353.

Ohkouchi, N., Kashiyama, Y., Kuroda, J., Ogawa, N., and Kitazato, H. (2006). The importance of diazotrophic cyanobacteria as primary producers during Cretaceous Oceanic Anoxic Event 2. *Biogeosciences* 3, 467–478. doi: 10.5194/bg-3-467-2006

Ohkouchi, N., Kuroda, J., and Taira, A. (2015). The origin of cretaceous black shales: a change in the surface ocean ecosystem and its triggers. *Proc. Jpn. Acad. Ser. B Phys. Biol. Sci.* 91, 273–291. doi: 10.2183/pjab.91.273

Ohkouchi, N., Nakajima, Y., Ogawa, N. O., Chikaraishi, Y., Suga, H., Sakai, S., et al. (2008). Carbon isotopic composition of the tetrapyrrole nucleus in chloropigments from a saline meromictic lake: a mechanistic view for interpreting the isotopic signature of alkyl porphyrins in geological samples. *Org. Geochem.* 39, 521–531. doi: 10.1016/j.orggeochem.2007.11.002

Ohkouchi, N., Nakajima, Y., Okada, H., Ogawa, N. O., Suga, H., Oguri, K., et al. (2005). Biogeochemical processes in the saline meromictic Lake Kaiike, Japan: implications from molecular isotopic evidences of photosynthetic pigments. *Environ. Microbiol.* 7, 1009–1016. doi: 10.1111/j.1462-2920.2005.00772.x

Popp, B. N., Takigiku, R., Hayes, J., Louda, J. W., and Baker, E. W. (1989). The post-Paleozoic chronology and mechanism of 13C depletion in primary marine organic matter. *Am. J. Sci.* 289, 436–454. doi: 10.2475/ajs.289.4.436

Reghizzi, M., Lugli, S., Manzi, V., Rossi, F. P., and Roveri, M. (2018). Orbitally forced hydrological balance during the messinian salinity crisis: insights from strontium isotopes (87Sr/86Sr) in the Vena del Gesso Basin (Northern Apennines, Italy). *Paleoceanogr. Paleoclimatol.* 33, 716–731.

Robinson, R. S., Kienast, M., Luiza Albuquerque, A., Altabet, M., Contreras, S., De Pol Holz, R., et al. (2012). A review of nitrogen isotopic alteration in marine sediments. *Paleoceanography* 27:A4203.

Rouchy, J. M., and Caruso, A. (2006). The messinian salinity crisis in the mediterranean basin: a reassessment of the data and an integrated scenario. *Sediment. Geol.* 188-189, 35–67. doi: 10.1016/j.sedgeo.2006.02.005

Roveri, M., Flecker, R., Krijgsman, W., Lofi, J., Lugli, S., Manzi, V., et al. (2014). The messinian salinity crisis: past and future of a great challenge for marine sciences. *Mar. Geol.* 352, 25–58. doi: 10.1016/j.margeo.2014.02.002

Ryan, W. B. (2009). Decoding the mediterranean salinity crisis. *Sedimentology* 56, 95–136. doi: 10.1111/j.1365-3091.2008.01031.x

Sachs, J. P., and Repeta, D. J. (1999). Oligotrophy and nitrogen fixation during eastern mediterranean sapropel events. *Science* 286, 2485–2488. doi: 10.1126/science.286.5449.2485

Sachs, J. P., Repeta, D. J., and Goericke, R. (1999). Nitrogen and carbon isotopic ratios of chlorophyll from marine phytoplankton. *Geochim. Cosmochim. Acta* 63, 1431–1441. doi: 10.1016/s0016-7037(99)00097-6

Sanger, J. E. (1988). Fossil pigments in paleoecology and paleolimnology. *Palaeogeogr. Palaeoclimatol. Palaeoecol.* 62, 343–359. doi: 10.1016/0031-0182(88)90061-2

Schaeffer, P., Harrison, W., Keely, B., and Maxwell, J. (1995). Product distributions from chemical degradation of kerogens from a marl from a miocene evaporitic sequence (Vena del Gesso, N. Italy). *Org. Geochem.* 23, 541–554. doi: 10.1016/0146-6380(95)00033-b

Schaeffer, P., Ocampo, R., Callot, H., and Albrecht, P. (1993). Extraction of bound porphyrins from sulphur-rich sediments and their use for reconstruction of palaeoenvironments. *Nature* 364, 133–136. doi: 10.1038/364133a0

Schaeffer, P., Ocampo, R., Callot, H. J., and Albrecht, P. (1994). Structure determination by deuterium labelling of a sulfur-bound petroporphyrin. *Geochim. Cosmochim. Acta* 58, 4247–4252. doi: 10.1016/0016-7037(94)90276-3

Scharek, R., Tupas, L. M., and Karl, D. M. (1999). Diatom fluxes to the deep sea in the oligotrophic North Pacific gyre at Station ALOHA. *Mar. Ecol. Prog. Ser.* 182, 55–67. doi: 10.3354/meps182055

Schouten, S., Breteler, W. C. K., Blokker, P., Schogt, N., Rijpstra, W. I. C., Grice, K., et al. (1998). Biosynthetic effects on the stable carbon isotopic compositions of algal lipids: implications for deciphering the carbon isotopic biomarker record. *Geochim. Cosmochim. Acta* 62, 1397–1406. doi: 10.1016/s0016-7037(98)00076-3

Schouten, S., Hartgers, W. A., Lòpez, J. F., Grimalt, J. O., and Sinninghe Damsteì, J. S. (2001). A molecular isotopic study of 13C-enriched organic matter in evaporitic deposits: recognition of CO2-limited ecosystems. *Org. Geochem.* 32, 277–286. doi: 10.1016/s0146-6380(00)00177-7

Schouten, S., Pavlovicì, D., Sinninghe Damsteì, J. S., and de Leeuw, J. W. (1993). Nickel boride: an improved desulphurizing agent for sulphur-rich geomacromolecules in polar and asphaltene fractions. *Org. Geochem.* 20, 901–909. doi: 10.1016/0146-6380(93)90101-g

Sinninghe Damsté, J. S., Frewin, N. L., Kenig, F., and De Leeuw, J. W. (1995). Molecular indicators for palaeoenvironmental change in a Messinian evaporitic sequence (Vena del Gesso, Italy). I: variations in extractable organic matter of ten cyclically deposited marl beds. *Org. Geochem.* 23, 471–483. doi: 10.1016/0146-6380(95)00040-l

Stauber, J. L., and Jeffrey, S. (1988). Photosynthetic pigments in fifty-one species of marine diatoms. *J. Phycol.* 24, 158–172. doi: 10.1111/j.1529-8817.1988.tb04230.x

Stiller, M., Rounick, J. S., and Shasha, S. (1985). Extreme carbon-isotope enrichments in evaporating brines. *Nature* 316, 434–435. doi: 10.1038/316434a0

Subramaniam, A., Yager, P., Carpenter, E., Mahaffey, C., Björkman, K., Cooley, S., et al. (2008). Amazon river enhances diazotrophy and carbon sequestration in the tropical North Atlantic Ocean. *Proc. Natl. Acad. Sci. U.S.A.* 105, 10460–10465. doi: 10.1073/pnas.0710279105

Sundararaman, P., and Boreham, C. J. (1993). Comparison of nickel and vanadyl porphyrin distributions of sediments. *Geochim. Cosmochim. Acta* 57, 1367–1377. doi: 10.1016/0016-7037(93)90078-b

Tayasu, I., Hirasawa, R., Ogawa, N. O., Ohkouchi, N., and Yamada, K. (2011). New organic reference materials for carbon-and nitrogen-stable isotope ratio measurements provided by center for ecological research, kyoto university, and institute of biogeosciences, Japan agency for marine-earth science and technology. *Limnology* 12, 261–266. doi: 10.1007/s10201-011-0345-5

Teranes, J. L., and Bernasconi, S. M. (2000). The record of nitrate utilization and productivity limitation provided by δ15N values in lake organic matter — A study of sediment trap and core sediments from Baldeggersee, Switzerland. *Limnol. Oceanogr.* 45, 801–813. doi: 10.4319/lo.2000.45.4.0801

Treibs, A. (1936). Chlorophyll and hemin derivatives in organic materials. *Angew. Chem.* 49, 682–686.

van Breugel, Y., Schouten, S., Paetzel, M., Ossebaar, J., and Sinninghe Damsteì, J. S. (2005). Reconstruction of δ13C of chemocline CO2(aq) in past oceans and lakes using the δ13C of fossil isorenieratene. *Earth. Planet. Sci. Lett.* 235, 421–434. doi: 10.1016/j.epsl.2005.04.017

Verne-Mismer, J., Ocampo, R., Callot, H., and Albrecht, P. (1988). Molecular fossils of chlorophyll c of the 17-nor-DPEP series. Structure determination, synthesis, geochemical significance. *Tetrahedron Lett.* 29, 371–374. doi: 10.1016/s0040-4039(00)80099-4

Wada, E. (1980). "Nitrogen isotope fractionation and its significance in biogeochemical processes occurring in marine environments," in *Isotope Marine Chemistry*, eds E. Goldberg, Y. Horibe, and K. Saruhashi (Tokyo: Uchida Rokakuho), 375–398.

Warren, J. K. (2010). Evaporites through time: tectonic, climatic and eustatic controls in marine and nonmarine deposits. *Earth Sci. Rev.* 98, 217–268. doi: 10.1016/j.earscirev.2009.11.004

Warren, J. K. (2016). *Evaporites: A Geological Compendium*. New York, NY: Springer, 1813.

Yoshimura, T., Kuroda, J., Lugli, S., Tamenori, Y., Ogawa, N. O., Jimeìnez-Espejo, F. J., et al. (2016). An X-ray spectroscopic perspective on Messinian evaporite from Sicily: sedimentary fabrics, element distributions, and chemical environments of S and Mg. *Geochem. Geophys. Geosyst.* 17, 1383–1400. doi: 10.1002/2015gc006233

Conflict of Interest Statement: The authors declare that the research was conducted in the absence of any commercial or financial relationships that could be construed as a potential conflict of interest.